Acc. Chem. Res. **2002,** *35,* 149−157

Micropattern Formation in Supported Lipid Membranes

JAY T. GROVES† AND STEVEN G. BOXER*,‡

Departments of Chemistry, Stanford University, Stanford, California 94305-5080, and University of California, Berkeley, California 94720

Received July 17, 2001

ABSTRACT

Phospholipid vesicles exhibit a natural tendency to fuse and assemble into a continuous single bilayer membrane on silica and several other substrate materials. The resulting supported membrane maintains many of the physical and biological characteristics of free membranes, including lateral fluidity. Recent advances, building on the supported membrane configuration, have created a wealth of opportunities for the manipulation, control, and analysis of membranes and the reaction environments they provide. The work reviewed in this Account, which can be broadly characterized as the science and technology of membrane patterning, contains three basic components: lateral diffusion control (barriers), membrane deposition techniques (microarrays), and electric field-induced lateral reorganization. Collectively, these preparative and analytical patterned membrane techniques offer a broad experimental platform for the study and utilization of lipid membranes.

Introduction

The phospholipid bilayer is arguably the definitive structural motif of living cells. In addition to compartmentalizing the cell, lipid membranes provide a two-dimensional fluid reaction environment in which orientational constraints, restricted component access, and long-range electrostatic forces strongly influence molecular interactions. Current models of cell membranes generally depict a dynamic and highly organized fluid mosaic exhibiting a considerable degree of lateral heterogeneity.[1−5] There is enormous interest in the study of membrane lateral structure since the spatial localization and cooperative rearrangement of membrane components is emerging as a critical aspect of numerous cellular processes, for example, immune recognition[6−11] and integrin signaling,[12−14] to mention only two. Despite the ubiquitous involvement of lipid membranes in biochemical processes, disproportionately little is known about the physical characteristics of membrane organization. This is partly due to the fact that membranes are notoriously difficult to control and manipulate, and because conventional structural methods are ill suited for characterizing a system with such a high degree of fluidity and attendant disorder. However, recent advances in the development of supported membrane systems provide an array of promising opportunities for the precise control and quantitative study of phospholipid membranes and the mechanisms by which they influence biochemical processes.

A supported membrane is generally defined as a single, continuous phospholipid bilayer on a solid or polymeric substrate and was originally developed for use in cell−cell recognition studies.[15−19] In 1984, Brian and McConnell created supported membranes containing the major histocompatibility (MHC) protein and demonstrated that these could effectively replace the antigen-presenting cell and elicit a specific immune response from living T lymphocytes.[15] Over the years, various studies of cell recognition and adhesion have greatly expanded upon this strategy (see, for example, refs 20−25). The remarkable ability of supported membranes to preserve specific biological function is beautifully illustrated by the recent observation of active immunological synapse formation between living T lymphocytes and supported membranes containing MHC and intercellular adhesion molecules (ICAM-1).[6]

Supported membranes can be assembled by spontaneous adsorption and fusion of unilamellar phospholipid vesicles with an appropriate substrate.[15,26] Alternative methods such as Langmuir−Blodgett dipping[16] or membrane spreading[27] can also produce high-quality supported membranes. Interactions between membranes and surfaces involve electrostatic and hydration forces as well as attractive contributions from long-range van der Waals forces. An energetic minimum tightly traps the membrane near the surface; alternatively, covalent tethering can been employed.[28] Supported bilayers are typically separated from the solid substrate by a thin (∼10 Å) film of water[29−31] and retain many of the properties of free membranes, including lateral fluidity. The fluidity is long range, with mobile components of both leaflets of the bilayer diffusing freely over the entire surface of the substrate.

The lateral fluidity of supported membranes is a key feature that distinguishes them from other surfaces. However, it presents an intrinsic difficulty in that membrane components are continually mixing. A pivotal realization was that barriers to lateral diffusion can be imposed on the supported membrane and used to partition it into corrals with well-defined geometry (Figure 1). Such barriers can be introduced into an existing membrane by manually scratching[32] or blotting away material from the membrane-coated surface.[33] Alternatively, par-

Steven Boxer received his B.S. from Tufts University and his Ph.D., under the guidance of Gerhard Closs, from the University of Chicago in 1976. He has been at Stanford since that time and is presently the Camille and Henry Dreyfus Professor of Chemistry. His research is at the interface of physical chemistry and biology. His interests include the mechanism of the early events in photosynthesis, electrostatics and dynamics in proteins such as heme proteins and green fluorescent protein, Stark spectroscopy, and biological membrane organization and function.

Jay Groves received a B.S. from Tufts University and a Ph.D., under the guidance of Steven Boxer and Harden McConnell, from Stanford University in 1998. He then spent a year as a visiting scholar at Academia Sinica in Taiwan. Upon returning to America, he became a Division Director's Fellow at the Lawrence Berkeley National Laboratory and later joined the faculty in the chemistry department at the University of California, Berkeley, in 2001. Groves's interests revolve around the physical properties of lipid membranes and their role in controlling biological processes such as cell recognition and signal transduction.

* Corresponding author. Phone: (650) 723-4482. Fax: (650) 723-4817. E-mail: Sboxer@stanford.edu.
† University of California, Berkeley.
‡ Stanford University.

10.1021/ar950039m CCC: $22.00
Published on Web 03/03/2002

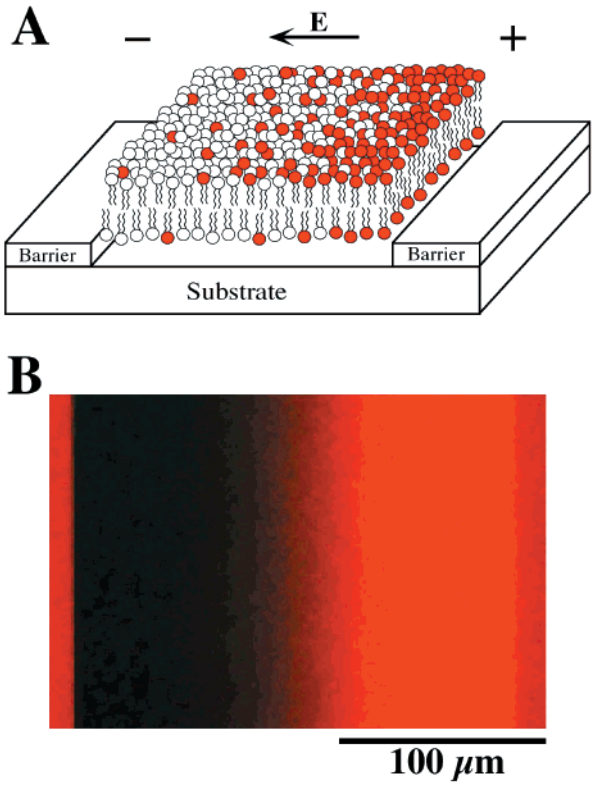

FIGURE 1. (A) Schematic diagram of a supported membrane; this membrane is confined by a pair of diffusion barriers which have been fabricated onto the supporting substrate. The membrane is separated from the substrate by a ~10 Å layer of water and the lipids diffuse freely. Electric fields can be used to induce rearrangement of charged membrane components, labeled in red. (B) Fluorescence image of a membrane corral (as in A) in which a laterally applied electric field maintains a steady-state concentration gradient of the negatively charged fluorescent lipid (1 mol % Texas Red) within a primarily egg-PC membrane.

titioning can be achieved by assembling membranes on prepatterned supports.[34,35] In all cases lipids exhibit uninterrupted diffusion within each corral, while there is no intermixing between separate corrals.

The geometric arrangement of diffusion barriers that constrain the membrane and determine its topology can be thought of as the primary level of patterning. As a secondary level of pattern formation, the composition of the membrane at different lateral positions can be varied. In the case of an array of isolated membrane corrals, for example, different lipid compositions or proteins can be deposited or flowed into individual corrals in the array, thus producing a mosaic pattern of fluid membrane elements, each with differing compositions.[34,36,37] Such membrane microarrays are proving useful in membrane discrimination studies[38] and multiplexed screening applications.

Another type of secondary patterning can be achieved by using external forces, such as those due to a tangentially applied electric field, to induce lateral reorganization within a fluid membrane mixture, also illustrated in Figure 1.[32,39] The rearrangement of membrane components after deposition offers a number of capabilities including directed concentration of lipids or proteins[40] and generation of continuous concentration gradients.

Electric field-induced reorganization of membranes can also be employed in a variety of analytical applications. The electrophoretic motion of lipids or proteins in the membrane and DNA molecules or even cells interacting with the membrane surface is analogous to conventional electrophoresis, except that the medium is a lipid bilayer rather than a hydrated gel or aqueous solution.[32,41] Field-induced drift can also be combined with an asymmetric labyrinth of microfabricated diffusion barriers that function as a geometrical Brownian ratchet.[42] When membrane components are electrophoretically driven through the labyrinth, molecules are sorted in the direction perpendicular to the field-induced motion on the basis of differences in size and/or charge. In addition to drift measurements, the ability to partition the membrane into isolated corrals allows a type of equilibrium electrophoresis. In this case, concentration gradients build up in the confined corrals until entropic and other intermolecular forces exactly balance the field-induced drift. The shape of the ensuing field-induced concentration profile reveals information about the clustering state of molecules in the membrane as well as providing quantitative characterization of subtle and transient interactions between membrane components.[39,43−45] Both experimental and theoretical aspects of these field-induced concentration profiles will be reviewed here.

Diffusion Barriers

A variety of techniques for fabricating supported membranes which are partitioned into a mosaic of isolated corrals by barriers to lateral diffusion have been developed. These fall into three basic categories: partitioning existing supported membranes, printing patches of supported membrane with fixed geometry, and prepatterning substrates to direct the subsequent membrane assembly.

The first technique developed to partition a supported membrane with an array of barriers to lateral diffusion involved mechanically scoring the membrane-coated substrate.[32] Leak-free barriers as narrow as a few microns can be created by scratching the supported membrane with a sharp object such as a pair of tweezers. Topographical scoring of the substrate contributes to the robustness of these so-called "scratch" barriers but is generally insufficient to produce a stable partition in a fluid membrane. Supported membranes are highly conformal and exhibit little difficulty flowing over contoured surfaces. Extremely sharp edges (radius of curvature $\ll$10 nm) such as those produced by reactive ion etching or deep abrasions on the surface are required to partition fluid membranes on the basis of substrate topography alone.

Effects involving hydration layers on the silica substrate have been found to play a substantial role in maintaining the stability of a scratch barrier.[46] Water molecules at a silica−buffer interface become ordered as the pH is raised, and this highly ordered hydration layer is a poor lubricant

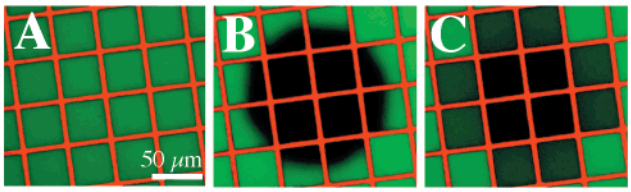

FIGURE 2. (A) Fluorescence image of corrals of supported membrane (green) partitioned by a grid of diffusion barriers (red). In this case, barriers were created by microcontact printing a grid of fibronectin onto a silica surface followed by membrane deposition. (B) A circular region covering a number of corrals has been photobleached by selective illumination. (C) After 20 min, diffusive mixing leads to uniform composition within each corral; the barriers prevent mixing between separate corrals. Figure adapted from Kam and Boxer, ref 51.

for a spreading membrane. Membranes spread or creep readily under mildly acidic conditions but cannot spread under basic conditions. Correspondingly, scratch barriers are quite stable under neutral or basic conditions but become unstable and can heal in a matter of minutes or hours, upon lowering of the pH.[47]

These observations can be exploited to create complex patterns by using a patterned polymer stamp such as poly(dimethylsiloxane) (PDMS) to "blot" away regions of a preassembled membrane.[33,48] If desired, the open glass region can be "caulked" by addition of polymers that bind to glass such as proteins.[49]

A second category of membrane patterning technology was discovered as a surprising corollary of membrane blotting. Blotting effectively "inks" the PDMS stamp, and the blotted membrane can then be transferred to a fresh glass surface. Alternatively (and preferably from a practical point of view), supported membranes can be assembled directly on an oxidized PDMS surface, and this can be used to print essentially any pattern of membrane on a glass substrate.[33,48]

A third fundamental method of imposing arrays of diffusion barriers on fluid membranes involves the use of substrates on which patterns of other (barrier) materials have been deposited prior to assembly of the supported membrane.[34] These patterned substrates are then used to guide the self-assembly of lipid vesicles into supported membranes with the desired pattern of diffusion barriers. The mechanism by which this process works is simple: lipid vesicles readily adsorb and fuse into a continuous supported membrane over the silica surface, whereas they do not form fluid membranes on the barriers. In fact, fluid membranes self-assemble on only a few substances, including a variety of glasses, silica, oxidized PDMS, and a few polymers.[50] Any substance that does not support fluid membranes can function as a barrier to lateral diffusion in the supported membrane. A wide range of materials including metals (Au, Al, Cr, Ti, etc., the latter presumably displaying oxide surfaces), metal oxides (for example, Al_2O_3 and TiO_2), and some polymers (including proteins patterned by microcontact printing) have proven to function as effective barriers[35,42,49,51] (Figure 2).

It is the chemical nature of the barrier material, not the topography, that blocks diffusion within the supported membrane. In the case of proteins such as bovine serum albumin, we have found that surface-adsorbed protein only a single monolayer in height (about 2−3 nm) is sufficient to pattern the bilayer. Lithographic processing techniques, developed extensively for the semiconductor industry, can be applied to pattern barrier materials on scales as small as tens of nanometers.

Membrane Microarrays

Supported membranes that have been partitioned into precisely defined arrays of fluid membrane corrals hold great potential for the study of cell membranes as well as the production of integrated biological−solid-state devices. For example, each corral can be filled with different components as a way of displaying a library of proteins or other molecules in a membrane environment.[38] This necessitates the ability to address individual corrals in the membrane array.

One strategy for modifying the individual corrals of a membrane microarray involves a secondary photolithographic step. The micropartitioned membrane itself is the substrate material for a spatially directed photochemical transformation that either eliminates functionality or activates the surface for attachment of some functionally interesting molecule (Figure 3A). This procedure is clean and can achieve very high spatial densities ($>10^6$ corrals/cm^2) but requires specific, photochemically active molecules.

A second approach to membrane microarray patterning was created by combining membrane microprinting with pre-existing fixed barriers on the surface. Variable fractions of the area within each prepatterned corral can be printed with a patch of supported membrane of one composition. The remaining open area within each corral can then be filled with a second composition by vesicle fusion from solution (Figure 3B). The newly formed membrane fuses with the existing printed membrane patch from the first step, and the compositions mix. In this way, any combination of fluid membrane components can be displayed in an array format.

A third method of membrane patterning exploits the fact that vesicle fusion is essentially irreversible. By flowing vesicle suspensions of different compositions under partial mixing conditions over a prepatterned glass surface, each micropatterned region will capture whatever composition is passing by (Figure 3C). This process combines the unique characteristics of a prepatterned surface to direct self-assembly, with flow and mixing, both of which can be controlled in sophisticated ways in microfluidic systems.[52]

It is also possible to directly deposit vesicle suspensions into individual corrals to produce membrane arrays.[36,38] Such direct deposit methods are perhaps the most general, since there is no intrinsic correlation between the composition of any two corrals in the membrane microarray. Each of the fabrication processes mentioned above de-

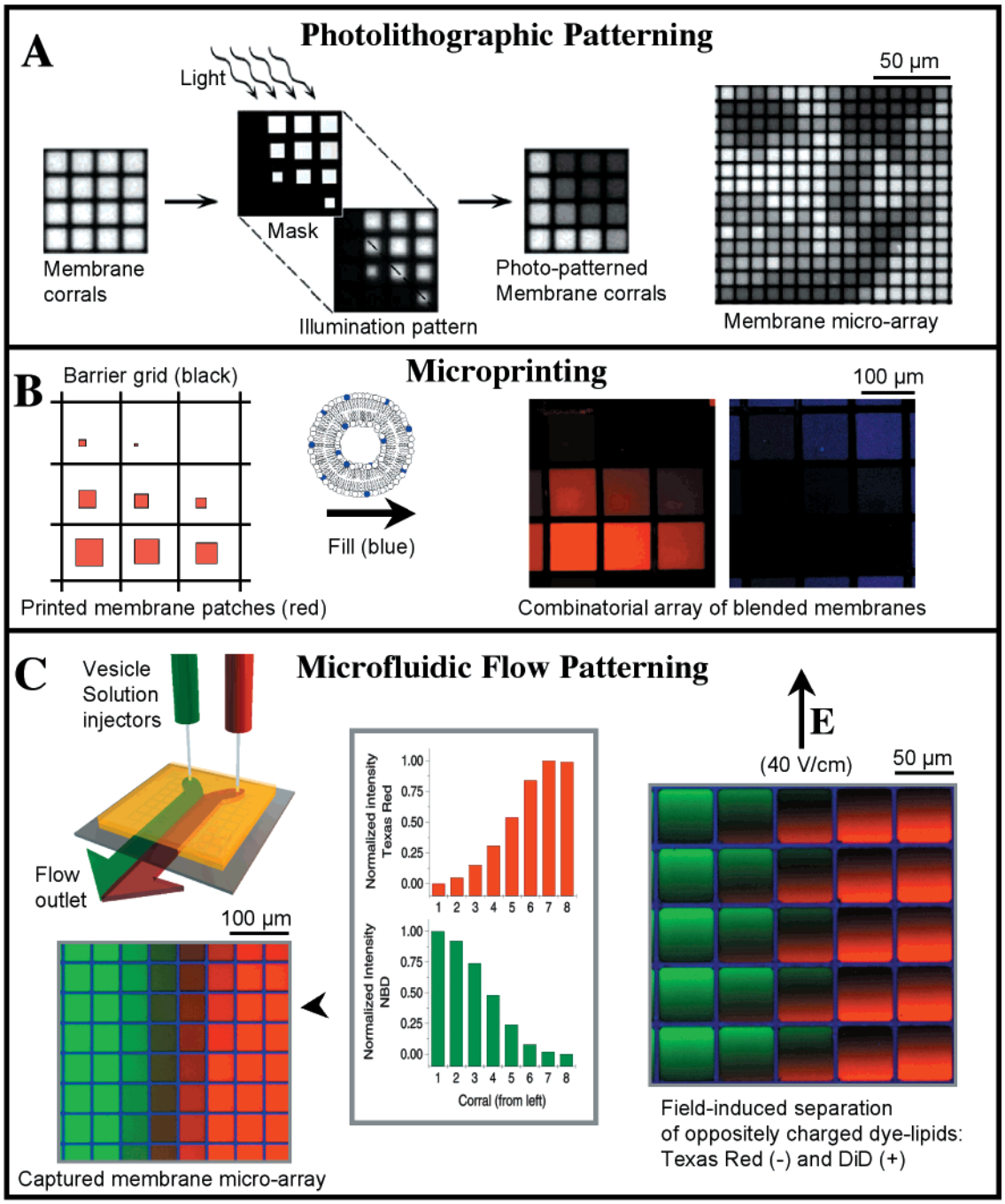

FIGURE 3. (A) A photomask is used to selectively expose each corral in an array with a specified dose of light. The light drives a chemical transformation: in this case, photobleaching of a fluorescent probe. The dose is determined by the fractional area of illumination; diffusive mixing leads to homogeneous compositions within each corral. A range of compositions is generated in a single photolithographic step. Adapted from Kung et al., ref 37. (B) A PDMS stamp is inked with membranes by vesicle fusion directly to the oxidized PDMS surface. This stamp is then used to deposit variably sized patches of supported membrane into an array of fixed corrals. The unfilled portions of each corral are then filled with a second membrane, thus leading to a composition array. In this example, various amounts of red membrane are printed, and a blue membrane is used to fill in. Images at right illustrate the relative compositions of Texas Red and Cascade Blue dye-labeled lipids in the nine corrals. Adapted from Hovis and Boxer, ref 48. (C) Two or more solutions of vesicles containing different molecules of interest (in this case Texas Red and green, DiD, dye-labeled lipids) are flowed over the surface of a prepatterned substrate. Vesicles adsorb irreversibly to the surface, fuse, and mix; thus, the composition in each region on the surface reflects the degree of mixing of the vesicles flowing over the surface. This gives rise to composition arrays (central panel). Fluidity is demonstrated by applying a lateral electric field (right panel). The dye-labeled lipids have opposite charges and are separated by application of the electric field. Adapted from Kam and Boxer, ref 52.

pends in one way or another upon the basic notion that the surface can be partitioned to direct the self-assembly of supported membranes, the vesicle fusion process itself, and the lateral fluidity within each corralled region.

Electric Field-Induced Reorganization

The fluid nature of supported membranes permits dynamic rearrangement of membrane components over macroscopic length scales. Application of an electric field tangent to a confined patch of fluid lipid membrane induces lateral reorganization of charged and uncharged components in the membrane mixture, as illustrated in Figure 1. Steady-state concentration gradients can be generated and manipulated with applied fields. The membranes remain fluid throughout this process, and the field-induced concentration gradients relax to uniformity by diffusive mixing when the field is turned off. Relatively low lateral field strengths (10−100 V/cm) induce micrometer-scale patterns that can be generated and shifted repeatedly without damaging the membrane or the diffusion barriers.

The combination of micropatterned membrane technology with electric field-induced reorganization provides a variety of novel analytical tools. Epifluorescence microscopy can be used to make quantitative measurements of the electrophoretic drift and equilibrium concentration profiles of fluorescently labeled components in supported membranes. Several experimental configurations will be discussed: drift velocity measurements, molecular separation in microfabricated labyrinths of diffusion barriers, and field-induced concentration profiles. Collectively, these techniques enable a wide range of experimental measurements that can reveal quantitative information about molecular interactions and organization within a lipid membrane environment.

Electrophoretic Drift. A tangential electric field imparts a net force on the charged components in a fluid membrane, causing them to drift with a characteristic electrophoretic drift velocity.[32,41] In the vicinity of a diffusion barrier, an image of the barrier will begin to drift along with this velocity upon application of the field. These images can be tracked over distances of more than 100 μm, allowing direct measurement of the drift velocity (Figure 4). Drift velocities for two GPI-linked proteins were measured to be 0.91 ± 0.05 μm/s (B7−2) and 0.57 ± 0.03 μm/s (CD-48) toward the negative electrode at a lateral field strength of 15 V/cm.[40] For comparison, drift velocities of negatively charged fluorescent lipid probes such as NBD-PE or Texas Red-PE in a 15 V/cm field are around 0.15 μm/s toward the positive electrode.[32,40]

The direction of the electrophoretic drift does not necessarily indicate the net charge of a molecule. A 15 V/cm lateral field typically induces a bulk electroosmotic flow in the flat capillary arrangement used for these experiments on the order of 100 μm/s. Frictional and hydrodynamic coupling to this flow contributes to the drift velocity of proteins and lipids in the membrane. Electroosmotic contributions reduce the drift velocity of negatively charged lipid probes by roughly 40%.[32,41] Unlike lipids, the protein complexes studied protrude far out of the membrane and are thus deeply immersed in the bulk electroosmotic flow. Electroosmotic effects can dominate the motion of membrane-associated proteins.[40]

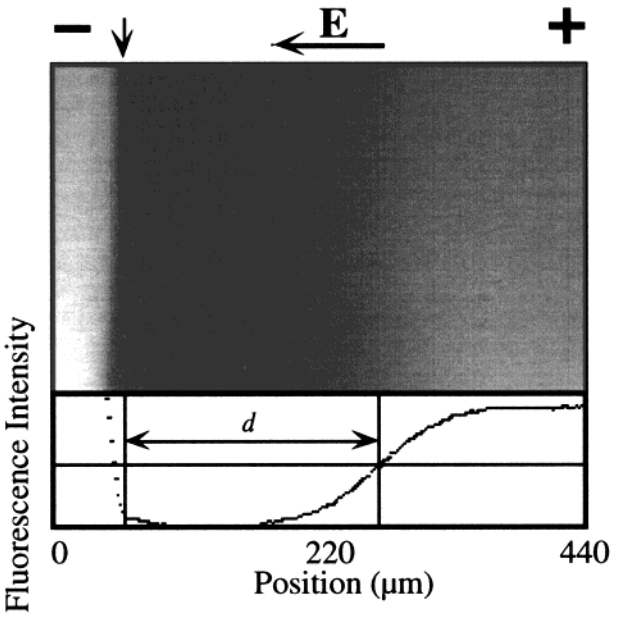

FIGURE 4. Drifting image of a barrier during approach to steady state. The scratch boundary is marked with a vertical arrow, and the field is in the direction indicated. The membrane consisted of pure egg-PC with 1% by mole Texas Red labeled lipid. The image was taken 600 s after a 20 V/cm field was first applied. Below is a trace of the fluorescence intensity (vertical average) across the image. Location of the midpoint, *d*, of this intensity profile allowed determination of the drift velocity.

Despite the complex origin of the composite electrophoretic force, f_i, on each component i, this is a well-defined quantity that can be determined directly from the drift velocity: $v_i = \eta_i f_i$. The mobility, η_i, can generally be obtained independently by measuring the diffusion coefficient, D_i, and making use of the Einstein relation, $D_i = \eta_i k_B T$. Reliable techniques, such as fluorescence recovery after photobleaching (FRAP), are available for measuring the diffusion coefficient of species in a fluid membrane.[53−55]

The drift velocity of molecules in a membrane is a characteristic property that can be used as a basis for molecular separations. A geometrical Brownian ratchet, consisting of a two-dimensional labyrinth of asymmetrical diffusion barriers through which a fluid is driven (Figure 5A), can exploit subtle differences in molecular mobility to achieve separation.[42] Percolation of molecules through the array of barriers results in a net lateral drift, perpendicular to the electrophoretic drift, which depends on the ratio of the electrophoretic drift velocity to the diffusion coefficient (Figure 5B). Negatively charged lipid molecules differing by a single charge were separated in a continuous fashion by this method. Variations on this strategy might be employed to separate more fragile membrane-associated molecules in a nearly native environment.

Equilibrium Concentration Profiles. Equilibrium concentration profiles within confined patches of a supported membrane are one of the most informative experimental observables provided by micropatterned membrane techniques. Field strengths of 10−100 V/cm typically produce concentration profiles with dimensions on the 100 μm size scale. Precise measurements of the concentration profiles

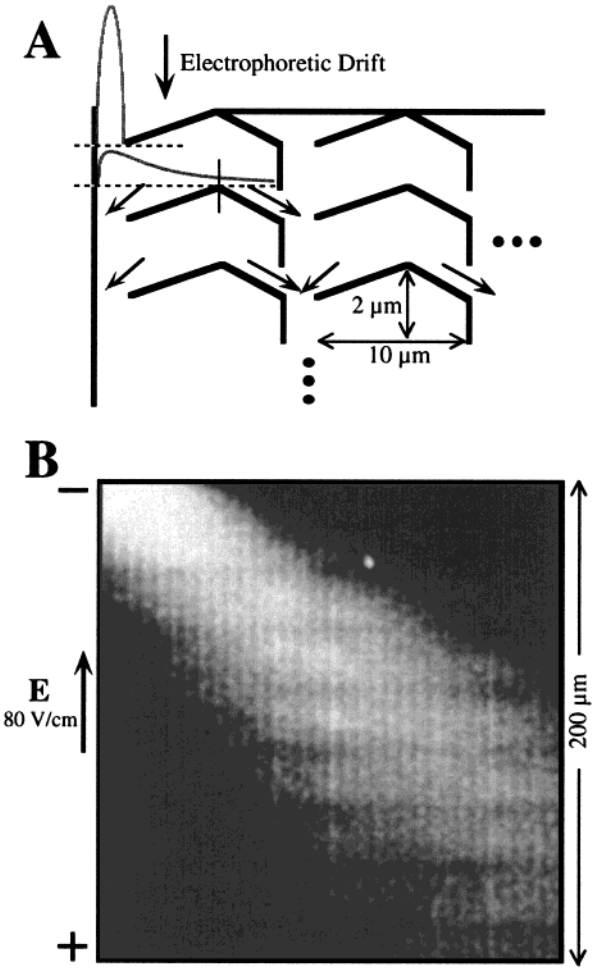

FIGURE 5. (A) Sketch of the layout of the geometrical Brownian ratchet projected into the plane of the support. A labyrinth of asymmetric diffusion barriers (Ti-oxide) is bordered by similar barriers which define an entrance to the ratchet. A fluid membrane is then assembled uniformly onto the remaining silicon oxide surface. During operation, membrane components are driven into the ratchet by an electric field and sieved, on the basis of lateral diffusion and drift velocity, as illustrated. (B) Fluorescence image after 2 h of operation, illustrating the direction of motion of negatively charged fluorescent dye-labeled lipids running through the Brownian ratchet (see ref 42 for details).

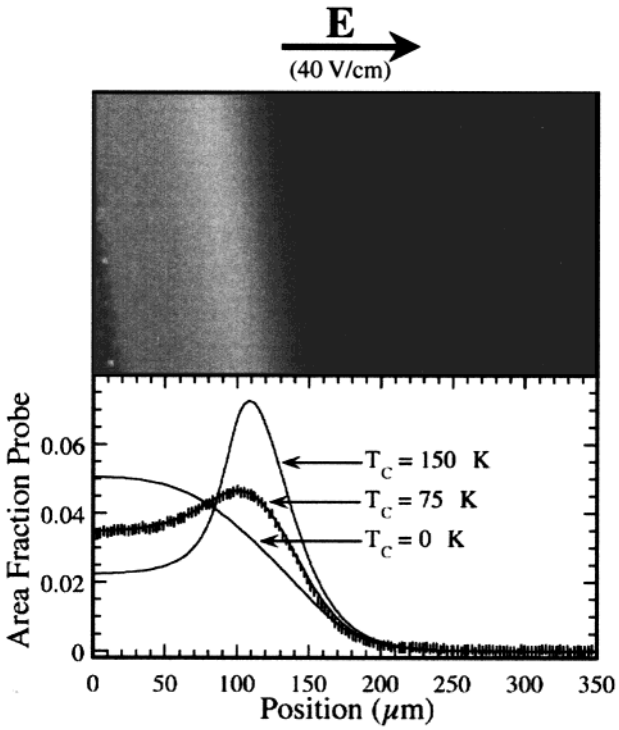

FIGURE 6. Experimental characterization of the mixing behavior of two lipid components by the dilute probe method. The upper panel contains an image of a steady-state concentration profile of the NBD-PE fluorescent lipid probe (1% by area) in a mixture of cardiolipin (14%) and egg-PC (85%). The negatively charged cardiolipin and NBD-PE have been driven toward the left side of this corral by the 40 V/cm electric field. A concentration gradient has built up along the scratch boundary, which is roughly at the zero position. A trace of the fluorescence intensity, which linearly correlates with the NBD-PE concentration, is plotted with vertical bars in the lower panel. Calculated profiles for different degrees of critical mixing are plotted with solid curves.

of fluorescently labeled membrane components can be made using epifluorescence microscopy.

The equilibrium concentration profile is determined by a balance between the relevant forces and effects of entropy (see eq 7 below). Experimental measurements have been in good agreement with calculations based on a thermodynamic model in which membrane components are characterized by their effective molecular areas, molecular charges, and the set of critical demixing coefficients (differential interaction energies) between each of the different species present (detailed below).

In a typical experiment, a dilute fluorescently labeled lipid is used to probe the mixing behavior of two other components in the bilayer membrane. Results from experiments on three-component supported membranes consisting of cardiolipin, egg-PC, and a fluorescent probe (NBD-PE) are illustrated in Figure 6. Both the cardiolipin and the NBD-PE probe are negatively charged and were driven toward the anode side of corralled sections of the membrane. Equilibrium distributions, such as the one shown here, can be reached in roughly 1 h under the conditions of these experiments.

A fluorescence image of the field-induced concentration profile of the probe is shown in the upper panel of Figure 6. At dilute levels, fluorescence from the probe is linearly proportional to its concentration; thus, the fluorescence intensity provides a direct measure of the probe distribution. The measured concentration of the probe (vertical bars) along with calculated profiles (solid lines) for varying degrees of critical demixing are plotted in the lower panel of Figure 6. These results suggest a critical demixing coefficient for cardiolipin/egg-PC mixtures corresponding to a critical temperature for spontaneous lateral phase separation, T_c, of 75 K. It is interesting to compare this result to similar experiments carried out on mixtures of phosphatidylserine (PS) and egg-PC where nearly ideal mixing ($T_c = 0$ K) was observed.[39] An advantage of the dilute probe method is that subtle changes in the concentration profiles of the major components can produce exaggerated differences in the probe concentration profile. This effect is particularly prominent in the

case at hand. Cardiolipin and egg-PC concentration profiles (inferred from the model) do not show as large or as distinctive a dependence on the critical demixing coefficient as was seen in the probe profile.[43] The field-induced concentration profile provides an observable that allows direct measurement of the propensity of a membrane to reorganize under the influence of lateral forces. As seen here, critical demixing effects persist in membranes even at temperatures and compositions far from a critical point.

Thermodynamic Model. The time-dependent reorganization of a membrane in response to lateral forces iscomputed from the set of chemical potentials $\{\mu_k\}$ as follows:

$$\frac{\partial \varphi_k}{\partial t} = \eta_k \nabla\cdot(\varphi_k \nabla \mu_k) \tag{1}$$

where φ_k is the area fraction of component k as a function of lateral position in the membrane. Equilibrium concentration profiles satisfy the condition $\nabla\mu_k = 0 \forall k$ and are independent of the mobility coefficients, η_k. The gradients of the chemical potentials used here are given by

$$\nabla\mu_k = k_B T\left(\frac{1}{\varphi_k}\frac{\partial \varphi_k}{\partial r} + \sum_i \left(\frac{A_{mi} - A_{mk}}{A_{mi}}\right)\frac{\partial \varphi_i}{\partial r}\right) + \frac{A_{mk}}{A_u}\sum_{i,j}\gamma_{ij}(\delta_i^k - \varphi_i)\frac{\partial \varphi_j}{\partial r} + A_{mk}\frac{\partial \Pi}{\partial r} - A_{mk} f_k + z_{mk} e \frac{\partial \psi}{\partial r} \tag{2}$$

where k_B is the Boltzmann constant, T is the temperature, r is the lateral position, A_u is the unit area of the lattice (equal to the smallest of the molecular areas), Π is the lateral pressure, ψ is the surface potential, and δ_i^k represents the Kronecker delta function defined as $\delta_i^k = \{1$ for $i = k$; 0 for $i \neq k\}$.[39,43−45] The long-range lateral forces acting on each component are represented by f_k in terms of force per unit area. Membrane components are characterized by their effective molecular areas (A_{mk}), molecular charges ($z_{mk}e$), and the set of critical demixing coefficients between each of the different species present $\{\gamma_{ij}\}$. This model employs Flory's approximation for the entropy of mixing in fluid mixtures consisting of differently sized particles.

Each γ_{ij} is directly related to the critical temperature in the corresponding binary mixture, thus offering a link between measurable parameters in simplified systems and the behavior of complex mixtures. In the case of two neutral components,

$$\gamma_{ij} = \frac{k_B T_c^{ij}}{2}\left(1 + \sqrt{\frac{A_{mj}}{A_{mi}}}\right)^2 \tag{3}$$

where A_{mi} is the larger of the two molecular areas.[43] Incorporating electrostatic effects from charged components, this relation becomes

$$\gamma_{ij} = \left[\frac{k_B T_c^{ij}}{2}\left(\frac{A_u}{A_{mi}}\left(\frac{1}{\varphi_i}\right) + \frac{A_u}{A_{mj}}\left(\frac{1}{1-\varphi_i}\right)\right) + \frac{A_u}{2}\left(\frac{z_{mi}e}{A_{mi}} - \frac{z_{mj}e}{A_{mj}}\right)\frac{\partial \psi}{\partial \varphi_i}\right]_{|\varphi_{icrit}} \tag{4}$$

evaluated at the critical composition (φ_{icrit}), which corresponds to the minimum value of the expression in square brackets over the interval $\{0 < \varphi_i < 1\}$.

Short-range electrostatic interactions such as those among the charged lipids in the membrane are computed using a continuum electrostatic model (Gouy−Chapman theory) to determine the local surface potential, ψ, from the membrane composition. The surface potential is related to the surface charge density by the Gouy equation:

$$\psi(\sigma) = \left(\frac{2k_B T}{ze}\right)\sinh^{-1}\left(\frac{\sigma z e L_D}{2k_B T \epsilon_w}\right) \tag{5}$$

where z is the valence of the symmetrical electrolyte solution, e is the elementary charge, ϵ_w is the dielectric constant of water, and L_D is the Debye length, defined as $L_D = (k_B T \epsilon_w / 2Iz^2e^2)^{1/2}$, with I denoting the ionic strength of the bulk solution. At low ionic strengths ($I \leq 1$ mM), the total surface charge density of the supported membrane is given by

$$\sigma = 2\sum_k \frac{z_{mk}e}{A_{mk}}\varphi_k + \sigma_0 \tag{6}$$

where the factor of 2 comes from the two leaflets of the bilayer membrane and σ_0 is the surface charge density on the substrate. By this definition, any net charge trapped in the water layer between the membrane and the support should be included in σ_0. In the high ionic strength of physiological environments, the Debye length is so short ($L_D < 1$ nm) that the two leaflets of the membrane may be treated independently,[56] thus eliminating the factor of 2 in eq 6; in this case σ_0 can be neglected as well.

Informative analytical solutions describing the equilibrium concentration profile can be obtained for binary systems. The equilibrium balance between applied forces and internal forces arising from concentration gradients is described by

$$\left(\frac{k_B T}{A_{m1}\varphi_1} + \frac{k_B T}{A_{m2}\varphi_2} - \frac{2\gamma}{A_u} + \left(\frac{z_{m1}e}{A_{m1}} - \frac{z_{m2}e}{A_{m2}}\right)\frac{\partial \psi}{\partial \varphi_1}\right)\frac{\partial \varphi_1}{\partial r} = f_1 - f_2 \tag{7}$$

Solutions are given by

$$r(\varphi_1) = \frac{k_B T \ln(\varphi_1)}{A_{m1}(f_1 - f_2)} + \frac{k_B T \ln(\varphi_2)}{A_{m2}(f_1 - f_2)} - \frac{2\gamma\varphi_1}{A_u(f_1 - f_2)} + \left(\frac{z_{m1}e}{A_{m1}} - \frac{z_{m2}e}{A_{m2}}\right)\frac{\psi(\varphi_1)}{(f_1 - f_2)} \tag{8}$$

which is the inverse of the concentration profile function $\varphi_1(r)$. A convenient feature of this representation is that critical demixing and electrostatic effects appear as strictly

additive terms. The boundary condition on eq 8 for a confined section of membrane requires that the total amount of each component remain constant:

$$\int_{A_T}\int \varphi_k \, dA = \bar{\varphi}_k A_T \tag{9}$$

where $\bar{\varphi}_k$ is the average composition of component k and A_T is the area of the confined region.

In the special case of a binary system with equally sized, neutral, non-interacting molecular components, eq 8 can be inverted:

$$\varphi_1(r) = \frac{1}{\exp(-A_{m1}(f_1 - f_2)(r - r_F)/k_B T) + 1} \tag{10}$$

This has the familiar form of a Fermi−Dirac distribution in which the energy function, $-A_{m1}(f_1 - f_2)r$, is the electrophoretic potential of component 1 relative to component 2. The boundary requirement is met by adjusting the positional parameter, r_F. Equation 10 may alternatively be expressed in terms of the drift velocity, $v_1 = \eta A_{m1}(f_1 - f_2)$, and diffusion coefficient, $D = \eta k_B T$. Noting that $v_1/D = A_{m1}(f_1 - f_2)/k_B T$, the concentration profile may be rewritten as follows:

$$\varphi_1(r) = \frac{1}{\exp(-v_1(r - r_F)/D) + 1} \tag{11}$$

Conclusion

The application of solid-state fabrication and soft lithographic technologies to the patterning and manipulation of lipid bilayer membranes has yielded a wealth of new techniques. Further developments in supported membrane technology are certain to continue, especially at the submicron length scale and with respect to incorporation of biological function. However, the most exciting advances lie ahead, as this emergent technology is applied to fundamental studies of cell membrane science and the engineering of integrated lipid membrane microdevices.

The authors thank their many co-workers who have contributed to this work, including Joshua Salafsky, Nick Ulman, Paul Cremer, Alexander van Oudenaarden, Li Kung, Jennifer Hovis, and Lance Kam, along with the inspiration and collaboration of Professor Harden McConnell. This work was supported in part by grants from the NSF Biophysics Program and by the MRSEC Program of the NSF under Award DMR-9808677. The Stanford Nanofabrication Facility (SNF) is gratefully acknowledged for support in fabrication.

References

(1) Jacobson, K.; Sheets, E. D.; Simson, R. Revisiting the fluid mosaic model of membranes. *Science* **1995**, *268*, 1441−1442.
(2) Simmons, K.; Ikonen, E. Functional rafts in cell membranes. *Nature* **1997**, *387*, 569−572.
(3) Mouritsen, O. G.; Kinnunen, P. J. K. Role of lipid organization and dynamics for membrane functionality. In *Biological membranes. A molecular perspective from computation to experiment*; Merz, J. K. M., Roux, B., Eds.; Birkhäuser: Boston, 1996; pp 463−502.
(4) Sheets, E. D.; Holowka, D.; Baird, B. Membrane organization in immunoglobulin E receptor signaling. *Curr. Opin. Chem. Biol.* **1999**, *3*, 95−99.
(5) Kurzchalia, T. V.; Parton, R. G. Membrane microdomains and caveolae. *Curr. Opin. Cell Biol.* **1999**, *11*, 424−431.
(6) Grakoui, A.; et al. The immunological synapse: A molecular machine controlling T cell activation. *Science* **1999**, *285*, 221−227.
(7) Davis, D. M.; et al. The human natural killer cell immune synapse. *Proc. Natl. Acad. Sci. U.S.A.* **1999**, *96* (26), 15062−15067.
(8) Wülfing, C.; Davis, M. M. A receptor/cytoskeletal movement triggered by costimulation during T cell activation. *Science* **1998**, *282*, 2266−2269.
(9) Viola, A.; Schroeder, S.; Sakakibara, Y.; Lanzavecchia, A. T Lymphocyte costimulation mediated by reorganization of membrane microdomains. *Science* **1999**, *283*, 680−682.
(10) Krummel, M. F.; Sjaastad, M. D.; Wülfing, C.; Davis, M. Differential Clustering of CD4 and CD3ζ during T-cell recognition. *Science* **2000**, *289*, 1349−1352.
(11) Qi, S. Y.; Groves, J. T.; Chakraborty, A. K. Synaptic pattern formation during cellular recognition. *Proc. Natl. Acad. Sci. U.S.A.* **2001**, *98* (12), 6548−6553.
(12) Giancotti, F. G.; Rouslahti, E. Integrin Signaling. *Science* **1999**, *285*, 1028−1032.
(13) Schoenwaelder, S. M.; Burridge, K. Bidirectional signaling between the cytoskeleton and integrins. *Curr. Opin. Cell Biol.* **1999**, *11*, 274−286.
(14) Schlaepfer, D. D.; Hunter, T. Integrin signaling and tyrosine phosphorylation: just the FAKs? *Trends Cell Biol.* **1998**, *8*, 151−157.
(15) Brian, A. A.; McConnell, H. M. Allogenic stimulation of cytoxic T cells by supported planar membranes. *Proc. Natl. Acad. Sci. U.S.A.* **1984**, *81*, 6159−6163.
(16) Tamm, L. K.; McConnell, H. M. Supported phospholipid bilayers. *Biophys. J.* **1985**, *47*, 105−113.
(17) McConnell, H. M.; Watts, T. H.; Weis, R. M.; Brian, A. A. Supported planar membranes in studies of cell−cell recognition in the immune system. *Biochim. Biophys. Acta* **1986**, *864*, 95−106.
(18) Watts, T. H.; McConnell, H. M. Biophysical aspects of antigen recognition by T cells. *Annu. Rev. Immunol.* **1987**, *5*, 461−475.
(19) Sackmann, E. Supported membranes: Scientific and practical applications. *Science* **1996**, *271*, 43−48.
(20) Chan, P.-Y.; et al. Influence of receptor lateral mobility on adhesion strengthening between membranes containing LFA-3 and CD2. *J. Cell Biol.* **1991**, *115* (1), 245−255.
(21) Tözeren, A.; et al. Micromanipulation of adhesion of a jurkat cell to a planar bilayer membrane containing lymphocyte function-associated antigen 3 molecules. *J. Cell Biol.* **1992**, *116* (4), 997−1006.
(22) Dustin, M. L.; et al. Visualization of CD2 interaction with LFA-3 and determination of the two-dimensional dissociation constant for adhesion receptors in a contact area. *J. Cell Biol.* **1996**, *132* (3), 465−474.
(23) Lawrence, M. B.; Springer, T. A. Leukocytes roll on a selectin at physiological flow rates: distinction from and prerequisite for adhesion through integrins. *Cell* **1991**, *65*, 859−873.
(24) Alon, R.; Hammer, D. A.; Springer, T. A. Lifetime of the P-selectin-carbohydrate bond and its response to tensile force in hydrodynamic flow. *Nature* **1995**, *374*, 539−542.
(25) Finger, E. B.; et al. Adhesion through L-selectin requires a threshold hydrodynamic shear. *Nature* **1996**, *379*, 266−269.
(26) Salafsky, J.; Groves, J. T.; Boxer, S. G. Architecture and function of membrane proteins in planar supported bilayers: a study with photosynthetic reaction centers. *Biochemistry* **1996**, *35*, 14773−14781.
(27) Rädler, J.; Strey, H.; Sackmann, E. Phenomenology and kinetics of lipid bilayer spreading on hydrophilic surfaces. *Langmuir* **1995**, *11*, 4539−4548.
(28) Raguse, B.; et al. Tethered lipid bilayer membranes: formation and ionic reservoir characterization. *Langmuir* **1998**, *14*, 648−659.
(29) Bayerl, T. M.; Bloom, M. Physical properties of single phospholipid bilayers adsorbed to micro glass beads. *Biophys. J.* **1990**, *58*, 357−362.
(30) Johnson, S. J.; et al. Structure of an adsorbed dimyristoylphosphatidylcholine bilayer measured with specular reflection of neutrons. *Biophys. J.* **1991**, *59*, 289−294.
(31) Koenig, B. W.; et al. Neutron reflectivity and atomic force microscopy studies of a lipid bilayer in water adsorbed to the surface of a silicon single crystal. *Langmuir* **1996**, *12* (5), 1343−1350.
(32) Groves, J. T.; Boxer, S. G. Electric field-induced concentration gradients in planar supported bilayers. *Biophys. J.* **1995**, *69*, 1972−1975.
(33) Hovis, J. S.; Boxer, S. G. Patterned barriers to lateral diffusion in supported lipid bilayer membranes by blotting and stamping. *Langmuir* **2000**, *16*, 894−897.
(34) Groves, J. T.; Ulman, N.; Boxer, S. G. Micropatterning fluid lipid bilayers on solid supports. *Science* **1997**, *275*, 651−653.

(35) Groves, J. T.; Ulman, N.; Cremer, P. S.; Boxer, S. G. Substrate−membrane interactions: Mechanisms for imposing patterns on a fluid bilayer membrane. *Langmuir* **1998**, *14* (12), 3347−3350.
(36) Cremer, P. S.; Yang, T. Creating spatially addressed arrays of planar supported fluid phospholipid membranes. *J. Am. Chem. Soc.* **1999**, *121*, 8130−8131.
(37) Kung, L.; Groves, J. T.; Ulman, N.; Boxer, S. G. Printing via photolithography on micropartitioned fluid lipid membranes. *Adv. Mater.* **2000**, *12* (10), 731−734.
(38) Groves, J. T.; Mahal, L. K.; Bertozzi, C. R. Control of cell adhesion and growth with micropatterned supported lipid membranes. *Langmuir* **2001**, *17* (17), 5129−5133.
(39) Groves, J. T.; Boxer, S. G.; McConnell, H. M. Electric field-induced reorganization of two-component supported bilayer membranes. *Proc. Natl. Acad. Sci. U.S.A.* **1997**, *94*, 13390−13395.
(40) Groves, J. T.; Wülfing, C.; Boxer, S. G. Electrical manipulation of glycan-phosphatidyl inositol-tethered proteins in planar supported bilayers. *Biophys. J.* **1996**, *71*, 2716−2723.
(41) Stelzle, M.; Miehlich, R.; Sackmann, E. Two-dimensional microelectrophoresis in supported lipid bilayers. *Biophys. J.* **1992**, *63*, 1346−1354.
(42) vanOudenaarden, A.; Boxer, S. G. Brownian ratchets: Molecular separations in lipid bilayers supported on patterned arrays. *Science* **1999**, *285*, 1046−1048.
(43) Groves, J. T.; Boxer, S. G.; McConnell, H. M. Electric field-induced critical demixing in lipid bilayer membranes. *Proc. Natl. Acad. Sci. U.S.A.* **1998**, *95*, 935−938.
(44) Groves, J. T.; Boxer, S. G.; McConnell, H. M. Electric field effects in multicomponent fluid lipid membranes. *J. Phys. Chem. B* **2000**, *104* (1), 119−124.
(45) Groves, J. T.; Boxer, S. G.; McConnell, H. M. Lateral reorganization of fluid lipid membranes in response to the electric field produced by a buried charge. *J. Phys. Chem. B* **2000**, *104*, 11409−11415.
(46) Cremer, P.; Boxer, S. G. Formation and spreading of lipid bilayers on planar glass supports. *J. Phys. Chem. B* **1999**, *103*, 2554−2559.
(47) Cremer, P. S.; Groves, J. T.; Kung, L. A.; Boxer, S. G. Writing and erasing barriers to lateral mobility into fluid phospholipid bilayers. *Langmuir* **1999**, *15*, 3893−3896.
(48) Hovis, J. S.; Boxer, S. G. Patterning and composition arrays of supported lipid bilayers by microcontact printing. *Langmuir* **2001**, *17*, 3400−3405.
(49) Kung, L. A.; Kam, L.; Hovis, J. S.; Boxer, S. G. Patterning hybrid surfaces of proteins and supported lipid bilayers. *Langmuir* **2000**, *16*, 6773−6776.
(50) Sackmann, E.; Tanaka, M. Supported membranes on soft polymer cusions: fabrication, characterization, and applications. *TIBTECH* **2000**, *18*, 58−64.
(51) Kam, L.; Boxer, S. G. Cell adhesion to protein-micropatterned supported lipid bilayer membranes. *J. Biomater. Res.* **2001**, *55*, 487−495.
(52) Kam, L.; Boxer, S. G. Formation of supported lipid bilayer composition arrays by controlled mixing and surface capture. *J. Am. Chem. Soc.* **2000**, *122*, 12901−12902.
(53) Axelrod, D.; et al. Mobility measurement by analysis of fluorescence photobleaching recovery kinetics. *Biophys. J.* **1976**, *16*, 1055−1069.
(54) Smith, B. A.; McConnell, H. M. Determination of molecular motion in membranes using periodic pattern photobleaching. *Proc. Natl. Acad. Sci. U.S.A.* **1978**, *75* (6), 2759−2763.
(55) Tamm, L. K.; Kalb, E. Microspectrofluoremetry of supported planar membranes. In *Molecular luminescence spectroscopy*; Schulman, S. G., Ed.; John Wiley & Sons: New York, 1993; pp 253−305.
(56) Bradshaw, R. W.; Robertson, C. R. Effect of ionic polarizability on electrodiffusion in lipid bilayer membranes. *J. Membr. Biol.* **1975**, *25*, 93.

AR950039M